Title: Dual-specific chimeric antigen receptor T cells and an indirect vaccine eradicate a variety of large solid tumors in an immunocompetent, self-antigen setting

Authors: Clare Y. Slaney[1,2], Bianca von Scheidt[1,2], Alexander J. Davenport[1,2], Paul A. Beavis[1,2], Jennifer A. Westwood[1,2], Sherly Mardiana[1,2], David C. Tscharke[3], Sarah Ellis[1,2], H. Miles Prince[1,2], Joseph A. Trapani[1,2], Ricky W. Johnstone[1,2], Mark J. Smyth[4], Michele W. Teng[5], Aesha Ali[1,2], Zhiya Yu[6], Steven A. Rosenberg[6], Nicholas P. Restifo[6], Paul Neeson[1,2], Phillip K. Darcy[1,2,7, †] and Michael H. Kershaw[1,2,7, †,*].

Affiliations: [1]Cancer Immunology Program, Peter MacCallum Cancer Center, Melbourne, Victoria, Australia. [2]Sir Peter MacCallum Department of Oncology, University of Melbourne, Parkville, Victoria, Australia. [3]John Curtin School of Medical Research, Australian National University, Canberra, Australia, [4]Immunology in Cancer and Infection Laboratory, QIMR Berghofer Medical Research Institute, Herston, Queensland, Australia. [5]Cancer Immunoregulation and Immunotherapy Laboratory, QIMR Berghofer Medical Research Institute, Herston, Queensland, Australia. [6]Center for Cancer Research, National Cancer Institute, National Institute of Health, Bethesda, MD, USA. [7]Department of Immunology, Monash University, Clayton, Australia. [†]Contributed equally.

*Correspondence should be addressed to M.H.K. or C.Y.K. Cancer Immunology Program, Peter MacCallum Cancer Center, 305 Grattan Street, Melbourne, Victoria, 3000, Australia. Email: michael.kershaw@petermac.org or clare.slaney@petermac.org. Telephone: (+613) 8559 7092 or (+613) 8559 5055. Fax: (+613) 8559 5039.

Keywords: Immunotherapy, cancer vaccine, breast cancer, colon cancer, sarcoma

Financial support: This work was supported by grants from the Cancer Council of Victoria, Australia (1066554), The Peter MacCallum Cancer Center Foundation, and the National Health and Medical Research Council (NHMRC) of Australia (1103352). CYS and PAB were supported by Postdoctoral Fellowships from the National Breast Cancer Foundation of Australia. AJD and SM received Postgraduate Scholarships from the Fight Cancer Foundation and University of Melbourne respectively. RWJ and MJS were supported by Senior Principal Research Fellowships from the NHMRC. MHK and PKD were supported by Senior Research Fellowships from the NHMRC. SE was supported by a New Investigator Grant from the NHMRC.

Conflict of interest statement: The authors declare no potential conflicts of interest

Translational Relevance

Adoptive transfer of T cells genetically modified to express a tumor-reactive chimeric antigen receptor (CAR) can mediate regression of some blood cancers. However, complete responses of a variety of large solid tumors in physiologically relevant models utilizing immunocompetent mice in a self-antigen setting have not been described before. In this study, we generate dual-specific CAR T cells that are able to respond to a potent immunogen through their T cell receptor and to a tumor antigen through their CAR. We demonstrate that adoptive transfer of dual-specific T cells together with vaccination mediates eradication of tumors of diverse histological origin. This approach also led to extensive expansion of dual-specific T cells and their massive infiltration of solid tumors, attributes important for optimal tumor responses. This study represents a major improvement in CAR T cell therapy, highly applicable to clinical translation.

ABSTRACT:

Purpose: While adoptive transfer of T cells bearing a chimeric antigen receptor (CAR) can eliminate substantial burdens of some leukemias, the ultimate challenge remains the eradication of large solid tumors for most cancers. We aimed to develop an immunotherapy approach effective against large tumors in an immunocompetent, self-antigen preclinical mouse model.

Experimental Design: In this study, we generated dual-specific T cells expressing both a CAR specific for Her2 and a TCR specific for the melanocyte protein (gp100). We used a regimen of adoptive cell transfer incorporating vaccination (ACTIV), with recombinant vaccinia virus expressing gp100, to treat a range of tumors including orthotopic breast tumors and large liver tumors.

Results: ACTIV therapy induced durable complete remission of a variety of $Her2^+$ tumors, some in excess of 150 mm^2, in immunocompetent mice expressing Her2 in normal tissues, including the breast and brain. Vaccinia virus induced extensive proliferation of T cells, leading to massive infiltration of T cells into tumors. Durable tumor responses required the chemokine receptor CXCR3 and exogenous IL-2, but were independent of IFN-gamma. Mice were resistant to tumor rechallenge, indicating immune memory involving epitope spreading. Evidence of limited neurologic toxicity was observed, associated with infiltration of cerebellum by T cells, but was only transient.

Conclusions: This study supports a view that it is possible to design a highly effective combination immunotherapy for solid cancers, with acceptable transient toxicity, even when the target antigen is also expressed in vital tissues.

INTRODUCTION

Adoptive cell transfer (ACT) is demonstrating exciting potential for cancer treatment. In ACT, autologous tumor-reactive T cells are generated in vitro before reinfusion to patients (1). Tumor-reactive T cells can be isolated from blood or tumor tissue of patients and expanded in vitro using stimulation with peptides and/or cytokines (1). The most impressive results of ACT in melanoma have objective responses in 52 of 93 patients (56%), with 20/93 patients achieving complete responses and 19 of those 20 patients with ongoing durable complete responses in excess of 5 years post-treatment (2). Studies at other centers around the world have also demonstrated durable complete responses in melanoma using ACT (3-5). Patients with EBV-associated lymphoproliferative disorders following bone marrow transplant can also benefit from ACT, with virtually all patients achieving complete resolution of disease after adoptive transfer of EBV-specific T cells (6).

However, despite these successes in melanoma and viral-induced malignancies, isolation of autologous T cells with reactivity against other cancer types is rare (7). Nevertheless, using genetic modification of patient lymphocytes, it is possible to generate tumor-reactive T cells against most malignancies, including solid cancers and those of the blood (8). Two main approaches of genetic modification involve genes encoding T cell receptor (TCR) or a chimeric antigen receptor (CAR). Both approaches can render T cells tumor-reactive, but the CAR approach, being non-MHC-restricted, is more widely applicable to a broader range of patients (9). The most advanced studies have utilized CARs specific for CD19 in clinical studies targeting B cell leukemias and lymphomas. The extraordinary potential of the CAR T cell approach as an effective treatment for cancer is supported by very high response rates of patients in these studies (10-13).

Despite the successes of CAR T cell therapy against these blood cancers, efficacy against solid cancers in patients has been much less. In over 80 patients suffering from a variety of solid cancers including renal cell carcinoma, neuroblastoma and cancers of the colon, ovary and prostate, durable complete responses have only been reported for 3 patients, all in neuroblastoma patients (8). Thus,

CAR T cell therapy can be effective against some blood cancers, but efficacy against common solid cancers is modest, at best.

The vast majority of previous reports using CAR T cells in mouse solid tumor models have utilized xenografts in immunodeficient mice, not expressing the target antigen in normal tissues, and that do not have the full complement of immune cells (14-16). Therefore, immunoregulation, tolerance induction and safety considerations do not closely represent that found in patients, making predictions about treatment efficacy and safety difficult.

Studies using CAR T cells targeting a self-antigen in immunocompetent mice are relatively rare, and have demonstrated the ability of ACT using genetically redirected T cells to inhibit growth of a limited range of small tumors in mice (17, 18), but larger tumors have not responded completely. In recent work, we combined ACT with a PD-1-neutralizing antibody and demonstrated enhanced antitumor effects against subcutaneous or mammary tumors (19). However, responses were again restricted to small tumors. Significant expansion or persistence of transferred T cells and their localization to solid tumors was not observed in these previous studies.

The reasons for the relatively low efficacy of CAR T cells against solid cancers are not clear, but could include poor persistence and expansion of transferred T cells, their low frequency of localization to tumors, and an immunosuppressive tumor microenvironment. To address these problems, in previous work, we initiated a novel approach to ACT involving the generation of dual-specific T cells (20, 21). In dual-specific T cells, an endogenous TCR specific for a strong immunogen (alloantigen, or influenza virus) provided the means for T cell proliferation (following immunization), while CARs specific for folate-binding protein (FBP) or Her2 provided the means for antitumor recognition and response. While CARs themselves do not generally enable robust T cell activation and expansion in response to solid tumors, T cell expansion was demonstrated using the strong immunogens. However, tumor responses and tumor localization of dual-specific T cells in these previous mouse models was low (T cell frequency <0.25% of total cells in tumor). We also reported

results of a Phase I clinical study using allo-reactive dual-specific CAR T cells, in which safety was demonstrated, although T cell persistence was short and T cell localization to tumors was below the level of detection (22).

Thus, in all our previous work, we have been unable to eradicate, or even significantly inhibit, large tumors using ACT. Indeed, reports of eradication of large solid tumors by immunotherapy in general in syngeneic immunocompetent mice are rare (23), and reports in the orthotopic, self-antigen setting, with rare exceptions, are virtually absent from the literature, and even then are restricted to a single tumor type (24). The identification of a therapeutic regimen able to mediate eradication of solid tumors of several different histologies in self-antigen immunocompetent mice remains a long sought after goal for cancer immunotherapy.

In our most recent attempts to maintain the activation and expansion of CAR T cells and improve their localization to tumors, we have tested another strong immunogen composed of live recombinant vaccinia virus encoding an antigenic peptide. Since the antigenic peptide was not tumor specific, we refer to the vaccine as "indirect". Thus, the approach involves Adoptive Cell Transfer Incorporating Vaccination (ACTIV) therapy. Here, we present a major advance in efforts to activate CAR T cells against large solid tumors in a syngeneic self-antigen setting using ACTIV therapy. ACTIV therapy induced expansion of CAR T cells and their localization to tumors, which led to eradication of large established solid tumors of several histologies in mice.

MATERIALS AND METHODS

Mice and cell lines

The C57BL/6-CAR (CAR) transgenic mice, generated on a C57BL/6 background, express an anti-Her2-CD28-CD3ζ chimeric antigen receptor under the control of the mouse vav promoter, as described previously (25). The C57BL/6-pMEL (pMEL) transgenic mice express a TCR specific for

human gp100 under the control of elements of the mouse TCRα and β promoters, as described previously (24). C57BL/6-CARaMEL mice were generated by crossing CAR and pMEL mice. C57BL/6-CARaMEL-Thy 1.1 mice were generated by crossing CARaMEL mice to C57BL/6-Thy 1.1 mice. C57BL/6-Her2 mice express human Her2 under the control of the whey acidic protein promoter, as described previously (26). All the above mouse strains were bred on site at the Peter MacCallum Cancer Center. C57BL/6-RAG1$^{-/-}$ mice were purchased from the Walter and Eliza Hall Institute of Medical Research, Parkville, Australia. Mice were ear-tagged, their numbers and their tumor measurements recorded, and randomly assigned to treatment groups. Tumor size was monitored by measurement along two perpendicular axes using calipers. Age- (8 -12 weeks) and gender-matched mice were used within each experiment. Individual mice were humanely killed when tumors reached 200 mm^2. Experiments on mice were performed with adherence to protocol E498 of the Animal Experimentation Ethics Committee at the Peter MacCallum Cancer Center and in accordance with the recommendations of the Victorian Bureau of Animal Welfare, Department of Primary Industries and National Health and Medical Research Council of Australia.

E0771 is a mouse breast cancer cell line (27), kindly provided by Dr Robin Anderson, Peter MacCallum Cancer Center, Melbourne, Australia. 24JK is a methylcholanthrene-induced fibrosarcoma (28), and MC38 is a chemically induced colon adenocarcinoma (29), both kindly provided by Dr Patrick Hwu, Surgery Branch, National Institutes of Health, Maryland, USA. All cell lines originated from C57BL/6 mice, and we had previously derived the Her2-expressing cell lines from the corresponding parental cells by retroviral transduction with cDNA encoding full length human Her2 expressed under control of the mouse stem cell virus LTR promoter (MSCV). 24JK-Her2 and MC38-Her2 were cultured in supplemented RPMI media as described previously (30), E0771-Her2 was cultured in supplemented DMEM, which enhanced adherence to flasks.

Recombinant vaccinia viruses

The vaccinia virus encoding human gp100 (VV-gp100) was constructed by insertion of a minigene containing the human $gp100_{25\text{-}33}$ epitope into the *F4L* gene encoding ribonucleotide reductase, and has been described previously (31). VV-OVA and VV-Flu contained an ER-targeted-SIINFEKL epitope from chicken ovalbumin and –SSLENFRAYV epitope from the influenza virus PA protein inserted into the thymidine kinase locus (gene *J2R*), as previously described (32, 33). Viruses were prepared from Hela S3 cells using sucrose density gradient centrifugation as described previously (34).

Tumor inoculation and treatment

Tumor cell lines were injected into Her2 transgenic mice. E0771-Her2 cells (5×10^5) were injected into the 4^{th} mammary fat pad to form orthotopic breast tumors. 24JK-Her2 fibrosarcoma cells (5×10^5) were injected subcutaneously. MC38-Her2 cells (5×10^5) were injected either subcutaneously or into the liver. For tumor rechallenge experiments, cells were injected into the corresponding contralateral site of tumor-free long-term surviving (>100 days) mice.

Adoptive cell transfer incorporating vaccination (ACTIV) therapy consisted of a lymphodepleting preconditioning regimen of 5 Gy whole body irradiation, followed approximately one hour later by intravenous injection of 1×10^7 mouse splenocytes, and after a further 2 hours by intravenous injection of 2×10^7 pfu vaccinia virus. Human recombinant IL-2 (Biological Resources Branch, National Cancer Institute, Frederick, MD, USA and Jiangsu Kingsley Pharmaceutical, China), at doses ranging from 100,000 to 500,000 IU, was administered intraperitoneally twice daily for 2 days. In some experiments individual subsets of T cells were purified according to manufacturer's instructions (Miltenyi Biotec) and 2.5×10^6 $CD8^+$ or 5×10^5 $CD4^+$ CARaMEL T cells (numbers typically present in 1×10^7 splenocytes) were substituted for splenocytes.

Microscopy, flow cytometry and cellular assays

Tissues were taken from non-treated or ACTIV-treated mice and snap frozen in liquid nitrogen or fixed in 10% neutral buffered formalin and embedded in paraffin. Sections were stained with a primary rat antibody specific for mouse CD8 (clone YTS 169.4, BioXcell, West Lebanon, NH) or mouse anti-human Her2 (clone 9G6.10, NeoMarkers, Freemont, CA). A secondary ImmPRESS HRP-conjugated anti-rat or anti-mouse IgG and Mouse-on-Mouse kit was used according to manufacturer's instructions (Vector Laboratories Ltd, Burlingame, CA) and counterstained with hematoxylin. The extent of apoptosis in tumors was assessed by antigen retrieval in 10 mM citrate buffer (pH6.0) using a pressure cooker followed by staining for cleaved caspase 3 using a specific antibody (9661, Cell Signalling Technology, Danvers, MA) or a rabbit polyclonal IgG isotype control, (AB27478, Abcam, Cambridge, MA, USA). Distribution of cleaved caspase 3 was visualized using a secondary ImmPRESS HRP-conjugated anti-rabbit IgG and sections were counterstained with hematoxylin. Sections were mounted in MM24 mounting media (Leica Biosystems, Australia) and scanned using an Olympus VS120 slide scanner (Olympus, Australia) equipped a x40 (UPLANSAPO NA0.95) objective and Allied Pike F-505C 16bit CCD color camera.

For flow cytometry, spleens were crushed in ACK lysis buffer, washed and resuspended in PBS. Tumors were first dissociated using collagenase IV (1 mg/ml, Worthington Biochemical, Lakewood, NJ) and DNAse I (30 units/ml, Sigma, Sydney, Australia) for 30 minutes at 37^{o}C, followed by washing and resuspension in PBS/0.5% FCS. Intracellular detection of IFN-γ was performed according to manufacturer's instructions (Clone XMG1.2, BD Biosciences, New Jersey, NJ).

To determine the ability of VV-gp100 to induce proliferation of dual-specific T cells, splenocytes (2 x 10^6 per well) from CARaMEL mice were incubated with gp100 peptide at indicated concentrations for 72 hours, before adding Alamar Blue for 4 hours and spectrophotometric analysis of fluorescence. Cytokine assays were performed using either serum or tumor digest using cytokine bead

array (Biolegend, San Diego, CA) or ELISA according to manufacturers' instructions. Cellular cytotoxicity was determined using ^{51}Cr release assay as previously described (35).

Neutralization of IFN-γ and CXCR3.

IFN-γ was neutralized by injection of an anti-IFN-γ monoclonal antibody (clone H22 BioXCell, West Lebanon, NH, USA). Injections of 200 μg per mouse were administered on the day of ACTIV treatment and 1, 4, 11 and 18 days later. CXCR3 blockade was accomplished using injections of 200 μg of an anti-CXCR3 monoclonal antibody (clone CXCR3-173, BioXCell) on the day of ACTIV therapy and then twice weekly for two weeks.

Statistical analyses

Tumor growth was compared using Mann-Whitney test (two groups) or one-way ANOVA (> two groups) for the curves or two-sided Student's t-test for individual time points. Mouse survival was compared using Mantel-Cox test. Comparisons of proliferation, cytotoxicity and T cell accumulation in spleens and tumors were performed using Student's t-test. A p-value of <0.05 was considered significant.

RESULTS

ACTIV therapy induces eradication of large solid tumors.

The tumor model system we employed to test ACTIV therapy against large established tumors involved injection of tumor cells, gene modified to express human Her2, into transgenic mice, which expressed human Her2 in normal breast and brain (26, 36). This unique system enabled testing of immunotherapy in an immunocompetent mouse strain, which was subject to the normal complement of

immune regulatory mechanisms. In addition, the presence of the target antigen as a self-antigen in normal tissues provided a physiologically relevant model enabling assessment of potential toxicities.

To provide a source of dual-specific T cells for ACT, we generated a transgenic mouse strain expressing a CAR specific for Her2 in leukocytes under the control of the vav promoter (25). This CAR mouse strain was bred onto the pMEL transgenic mouse strain, expressing a TCR specific for the premelanosome protein, gp100 (24). This novel hybrid mouse strain, expressing both a CAR and pMEL TCR in T cells, was referred to as the CARaMEL mouse strain, and provided a source of dual-specific T cells.

Consistent with our hypothesis that ACTIV therapy would enable expansion of T cells and their activation and acquisition of cytolytic ability, we first demonstrated the ability of T cells from CARaMEL mice to proliferate in response to gp100 (**Supplementary Fig. S1A**). The dual specificity of CARaMEL T cells was evident from their ability to secrete IFN-γ in response to both gp100 and Her2 (**Supplementary Fig. S1B**). Dual-specific T cells were also able to lyse tumor cells expressing either Her2 or gp100 (**Supplementary Fig. S1C**).

In our initial experiments to test the efficacy of ACTIV therapy against large established tumors, we injected the E0771-Her2 breast cancer cell line orthotopically into the mammary fat pad of C57BL/6-Her2 mice, and began ACTIV therapy, or variations lacking individual components, two weeks later when tumors were large, some in excess of 150 mm^2. The complete ACTIV therapy regimen involved a lymphodepleting preconditioning procedure of 5 Gy irradiation, followed on the same day by intravenous injection of 1 x 10^7 splenocytes from CARaMEL mice, which typically contained approximately 2 x 10^6 $CD8^+$ dual-specific CARaMEL T cells. Also included in the ACTIV regimen was 2 x 10^7 plaque-forming units of live vaccinia virus (VV) encoding human gp100 (VV-gp100) delivered intravenously approximately 2 hours after T cells, which was followed by

intraperitoneal injection of 4 doses of recombinant human IL-2 spaced approximately 12 hours apart at 500,000 IU per dose.

The growth of large tumors was significantly inhibited in all mice receiving the full ACTIV regimen (**Fig. 1A**). Observations of tumor growth in individual mice demonstrated that even tumors in excess of 150 mm^2 could respond completely to ACTIV therapy (**Fig. 1B,C**). Strikingly, over 75% of tumors were eradicated, leading to long term survival (**Fig. 1D**). Tumors in mice with ACTIV therapy lacking vaccine, or with pMEL T cells lacking CAR, were slowed in growth (**Fig. 1A**) but tumors eventually progressed and all mice succumbed to disease with only a modest increase in survival (**Fig. 1D**). A crucial role for the interaction between CAR and Her2 antigen was also supported by the observation that ACTIV therapy was less effective at inhibiting growth of Her2-negative tumors (**Fig. 1F**). The necessity for interaction between CAR and Her2 for tumor inhibition was also apparent in an experiment using a mixture of Her2-positive and Her2-negative tumor cells, which demonstrated the outgrowth of Her2-negative cells in ACTIV-treated mice (**Fig. 1G**). Taken together, these data demonstrated that ACTIV therapy lacking specific T cells or vaccination was not able to eradicate tumors. In mice receiving ACTIV therapy lacking IL-2, tumors initially responded similarly to those in mice receiving the full ACTIV regimen (**Fig. 1A**), but tumors eventually progressed in the majority of mice and long term survival was significantly less than mice receiving ACTIV therapy (**Fig. 1D**).

Since the transfer of splenocytes from CARaMEL mice contained a mixture of CAR-expressing leukocytes including both $CD4^+$ and $CD8^+$ T cells, we next sought to determine the contribution from individual leukocyte subsets. Tumors in mice receiving purified $CD8^+$ CARaMEL T cells as part of their ACTIV therapy responded similarly to those in mice receiving bulk CARaMEL splenocytes, whereas mice receiving purified $CD4^+$ CARaMEL T cells derived limited benefit (**Fig. 1E**). Similar antitumor activity was observed in mice receiving ACTIV therapy incorporating either $CD8^+$ T cells or a combination of $CD8^+$ and $CD4^+$ T cells. These results indicated that $CD8^+$ CARaMEL T cells, able to respond through both their CAR and TCR, were necessary and sufficient for effective therapy and were

the predominant effector cell in splenocytes. For ease of treatment, CARaMEL splenocytes were used in ACTIV therapy for subsequent experiments.

To gain further insight into the requirement for IL-2, we performed a dose titration experiment including various doses of IL-2 in the ACTIV treatment regimen. Significant numbers of long term surviving mice were only obtained using the higher doses of 250,000-500,000 IU twice daily for two days (**Supplementary Fig. S2A,B**). A role was identified for IL-2 in enhancing the proliferation of CARaMEL T cells as demonstrated *in vitro* (**Supplementary Fig. S2C**) and *in vivo* in combination with vaccination (**Supplementary Fig. S2D,E)**. While the individual contribution of IL-2 alone to T cell infiltration of tumor is not clear, the contribution of vaccination to antitumor activity of CARaMEL T cells is greater than the contribution from IL-2, as seen in Fig. 1A and Fig.1D. Thus, all tumors responded to just a single round of ACTIV therapy, and the majority of tumors regressed completely.

A range of solid tumor types respond to ACTIV therapy.

To determine the efficacy of ACTIV therapy against tumors of other histological origin, mice bearing subcutaneous 24JK-Her2 murine sarcoma received ACTIV therapy or control treatments. All tumors in ACTIV treated mice responded, and tumors were eradicated in 6 of 7 mice (**Fig. 2A**). To extend the therapy to other tumor types, MC38-Her2 mouse colon carcinomas were formed by subcutaneous injection, or by injection directly into the liver to establish a discreet, large intrahepatic mass. Again, ACTIV therapy eradicated tumors (**Fig. 2B-E**), whereas treatments lacking some components were less effective. Similarly to ACTIV therapy against E0771-Her2 tumors, optimal antitumor effects against 24JK-Her2 and MC38-Her2 were not achieved when the pMEL TCR was absent from transferred T cells (Supplementary Fig. S3). A crucial role for the CAR in tumor growth inhibition and eradication was evident from the reduced inhibition of Her2-positive tumors in the absence of CAR (**Fig. 2A,B**), Further support for the role of the CAR in antitumor activity was

provided by the observation that the ACTIV-mediated antitumor response was not significant for Her2-negative tumors (**Fig. 2F,G**). Interestingly, subcutaneous MC38-Her2 tumors responded better to VV-gp100 + pMEL than to CARaMEL T cells alone, suggesting that virus-mediated inhibition of tumor growth is a significant contributor to effective ACTIV therapy. Remarkably, all mice with established liver tumors survived long term after ACTIV therapy with no evidence of liver disease upon necropsy, whereas tumors progressed rapidly in non-treated mice, with large liver tumors and peritoneal spread evident (**Fig. 2E**). Therefore, the impressive efficacy of this approach was evident across four tumor model systems.

A specific vaccinia virus, TCR and CAR are necessary for optimal effect

To gain an understanding of the contribution from vaccinia virus, we substituted recombinant vaccinia virus expressing gp100 (VV-gp100) with recombinant vaccinia viruses expressing either ovalbumin (VV-OVA) or the polymerase acidic protein (PA) of influenza virus (VV-Flu). Although VV-OVA and VV-Flu had a modest effect on tumor growth, the most effective treatment required VV-gp100, which had the capacity to stimulate CARaMEL T cells through their TCR (**Fig. 3A**). This indicated that specific activation and expansion of dual-specific T cells through their TCR was necessary to achieve optimal antitumor activity.

In addition, therapy was ineffective when CAR T cells expressing an OT1 TCR specific for ovalbumin (CAROT T cells) were substituted for CARaMEL T cells, providing more support for the importance of the gp100-specific TCR. Furthermore, an experiment in which the CAR and TCR were present on separate T cells demonstrated that both of these antigen receptors needed to be on the same cell (**Fig. 3B**), further suggesting that activation and expansion of tumor-specific T cells was necessary for effective therapy.

Indeed, when tissues were taken from treated mice, extensive proliferation of CARaMEL T cells was observed in the spleens of mice receiving VV-gp100 compared to those receiving no virus

(**Fig. 4A**). Furthermore, extensive infiltration of tumor by CARaMEL T cells followed their expansion in the periphery (**Fig. 4B**). The remarkable increase in T cell infiltrate afforded by VV-gp100 was also evident from histological examination of tumors (**Fig. 4C**). T cell infiltration into tumor was independent of CAR expression, since T cells expressing the pMEL TCR alone also accumulated in tumors (**Fig. 4E**).

To gain further mechanistic insight into ACTIV therapy, we investigated the effect of therapy on cellular and molecular components of the tumor microenvironment. Strikingly, tumor-infiltrating CARaMEL T cells expressed high levels of intracellular IFN-γ when isolated from tumors 5 days after transfer, whereas most T cells isolated from spleen expressed no IFN-γ (**Fig. 4D**).

IFN-γ was also detected in dissociated tumors (**Supplementary Fig. S4A**). Apoptosis of tumor cells was also evident on Day 5 after ACTIV treatment (**Supplementary Fig. S4B**). Together, these data suggested that CARaMEL T cells contributed to therapy through a robust response specifically within the tumor. However, it is unknown at this stage if this was mediated solely against Her2 through the CAR or against VV-gp100 through the TCR or both.

However, in further mechanistic studies, we neutralized IFN-γ using a monoclonal antibody, and found that ACTIV therapy was still highly effective against established tumors (**Supplementary Fig. S4C**). This suggested that there were other mechanistic contributors to T cell function, and/or an increased contribution from vaccinia virus in the absence of the anti-viral function of IFN-γ. Indeed, the appearance of small lesions on the tails of treated mice was observed when IFN-γ was neutralized, indicating enhanced viral activity.

Additional insight into molecular contributors to therapy was gained by blocking the T cell-associated chemokine receptor, CXCR3. The survival of mice following ACTIV therapy was significantly reduced after CXCR3 blockade (**Supplementary Fig. S4D**), suggesting that this receptor was important in T cell trafficking during ACTIV therapy. Support for CXCR3 blockade acting

directly on T cells was provided by the observation that CXCR3 was expressed on activated CARaMEL T cells (**Supplementary Fig. S4E**). In addition, a role for CXCR3 in CAR-independent accumulation of T cells in tumor was supported by similar expression of CXCR3 on activated T cells lacking CAR expression (**Supplementary Fig S4E)**.

ACTIV therapy generates a memory response in surviving mice.

An important aim of immunotherapy should be to establish immune memory to protect against tumor recurrence. The existence of immune memory was supported by persistence of CARaMEL T cells for >100 days in lymph nodes and spleen of long term surviving mice (**Supplementary Fig. S5A,B**). CARaMEL T cells in surviving mice also expressed high levels of CD62L and CD44, consistent with a memory T cell phenotype (**Supplementary Fig. S5C**). To determine if an anti-tumor immune memory response could be mediated by ACTIV therapy, we rechallenged long term surviving mice with tumor cells in the contralateral site greater than 100 days following initial treatment. Mice that had rejected E0771-Her2 or MC38-Her2 or 24JK-Her2 were completely resistant to rechallenge with the same cells (**Fig. 5A-C**). Interestingly, surviving mice were also partially resistant to rechallenge with parental tumor cell lines lacking expression of Her2, suggesting that epitope spreading had occurred during the initial response leading to tumor-reactive T cells of other specificities (**Fig. 5D-F**). These data also suggested that the CAR played a role in protection against tumor rechallenge, since long-term survivors of Her2-expressing tumors were totally resistant to rechallenge with the same Her2-expressing tumor (Fig. 5A-C) but only partially resistant to rechallenge with tumor cells lacking expression of Her2 (Fig. 5D-F).

To determine the relative contribution of Her2 and other epitopes to immune memory, we rechallenged mice that had rejected E0771-Her2 with either MC38-Her2 or 24JK-Her2. In both cases, some protection against tumor growth occurred, but was only partial (**Fig. 5G,H**). MC38 and 24JK lacking Her2 expression grew at similar rates in naïve mice and those that had rejected E0771-Her2

(**Fig. 5I,J**). These data suggested that Her2-specific immune memory alone is not sufficient for complete protection.

ACTIV therapy can induce transient responses against Her2$^+$ normal tissues

The mouse model we used in this study provides a stringent test of treatment efficacy and potential toxicities in a self-antigen setting, where the target antigen is also expressed in some normal tissues, which is often the case in patients. Mice used in our study expressed human Her2 in normal breast and the molecular layer of the cerebellum (17, 26). Mice receiving ACTIV therapy showed some signs of transient toxicity, beginning approximately 5 days after treatment, manifested by weight loss, lethargy and unsteady gait, whereas mice receiving treatments lacking VV or T cells or IL-2 did not exhibit signs of toxicity.

In patients, toxicities following rapid regression of large tumor burdens include cytokine release syndrome (CRS) (37). CRS resulting from accumulation of cytokines including interferons and IL-6, can lead to hypotension, neurologic disturbances and pulmonary edema, and can be managed with corticosteroids or Tocilizumab (10). However, serum levels of murine IFN-γ and IL-6 and other cytokines in treated mice were relatively low (<100 pg/ml IL-6) (**Supplementary Fig. S6A**) in comparison to those associated with CRS (>1000 pg/ml IL6) (38), suggesting that CRS did not play a major role in the observed toxicity.

To provide a rigorous test of toxicity against breast, we used lactating mice, which express higher levels of mammary Her2 than non-lactating mice (26). T cells were found infiltrating breast tissue of ACTIV-treated mice (**Fig. 6A**) but not naive mice (**Fig. 6B**). The extent of T cell accumulation correlated with a high level of Her2 expression, since a much reduced level of infiltrate was present in the breasts of non-lactating mice (**Fig. 6C**), where Her2 expression was reduced compared to lactating mice.

To gain further insight into toxicity, we recovered the brains from non-treated and ACTIV-treated mice and performed immunohistochemistry to determine whether treatment provoked T cell infiltration into Her2-expressing normal tissues. T cells were absent from the brains of non-treated mice (**Fig. 6D**), but a T cell infiltrate was observed in the molecular layer of the cerebellum in ACTIV-treated mice, which extended into the granular layer (**Fig. 6E**). T cell infiltration was also observed in other areas of the brain, but to a much lesser degree (**Fig. 6F**). Since the cerebellum is important in maintaining coordination, it seemed likely this cerebellar inflammation was responsible for the observed unsteady gait of mice.

To determine the role of Her2 expression on toxicity and T cell infiltration into the brain, we treated $Her2^{+}$ tumor-bearing $RAG1^{-/-}$ mice with ACTIV therapy. $RAG1^{-/-}$ mice were chosen since mouse tumors expressing human Her2 will grow in this immunodeficient strain, unlike in wild type C57BL/6 mice which reject $Her2^{+}$ tumors. In addition, $RAG1^{-/-}$ mice lack expression of Her2 in the brain (**Fig. 6G**), unlike Her2 transgenic mice, which express substantial amounts in the molecular layer and Purkinje cells (**Fig. 6H**). A much reduced T cell infiltrate was observed in the brains of ACTIV-treated $RAG1^{-/-}$ mice (**Fig. 6I**) compared to that observed in Her2 transgenic mice, suggesting that Her2 expression played a role in the accumulation of large numbers of T cells in the brain.

Remarkably, despite the significant T cell infiltrate in the brain, ACTIV-treated Her2 mice recovered fully by Day 9 after treatment, with resolution of both lethargy and unsteady movement. In addition, histological examination greater than three months later demonstrated that brain tissue had returned to normal, exhibiting normal appearance of the molecular layer, granular layer and Purkinje cells of the cerebellum (**Fig. 6J, Supplementary Fig. S6B**). This resumption of normal tissue morphology was despite the persistence of CARaMEL T cells in lymph nodes and spleen greater than 100 days after tumor eradication. Furthermore, no ACTIV-mediated toxicity and no associated weight loss was observed in $RAG1^{-/-}$ mice (**Fig. 6K**), despite equivalent efficacy of ACTIV therapy in $RAG1^{-/-}$ mice (**Fig. 6L**).

DISCUSSION:

Eradication of large burdens of orthotopic solid tumors by immunotherapy in a syngeneic setting is extremely rare (23, 24), and we are not aware of any descriptions of an immunotherapeutic strategy able to eradicate established tumors of several different histologies in a self-antigen immunocompetent setting. In this study, we generated dual-specific T cells and used them in combination with an indirect viral vaccine in an immunotherapy regimen against established tumors in mice. ACTIV therapy, which included preconditioning, IL-2, dual-specific T cells and recombinant vaccinia, was highly effective in several tumor models including orthotopic breast cancer, subcutaneous sarcoma, and colon carcinoma present as large liver masses.

The dual-specific nature of the T cells enabled them to respond to tumor through a CAR, and expand in response to a vaccine through a TCR. The CAR was required for tumor eradication, since treatment using vaccine in combination with T cells lacking the CAR was unable to induce complete tumor responses. In this study, we made use of T cells from transgenic mice as a convenient source of effector cells without the need for genetic transduction. However, previous studies have demonstrated the feasibility of transducing primary T cells and manipulating their phenotype for adoptive transfer(39-41), which supports the translational potential of this approach.

We found that inclusion of $CD8^+$ CARaMEL T cells alone in the ACTIV regimen was sufficient for treatment efficacy, suggesting that the mechanism was largely independent of $CD4^+$ T cell help. CD4-independent CD8 T cell responses have been described previously in cancer and other disease settings (42, 43). However, although mice originally received lymphodepleting preconditioning, we cannot rule out a contribution from subsequent repopulation by endogenous $CD4^+$ T cells.

The recombinant strain of vaccinia used in this study contained a human gp100 minigene incorporated into the viral locus encoding a ribonucleotide reductase gene, effectively rendering the

virus deficient in this gene (31), resulting in attenuation of virulence and the potential gain of oncolytic potential (44). The virus had the ability to induce activation and proliferation of CARaMEL T cells, and expansion of T cells and their accumulation in tumors was demonstrated. Thus, the recombinant vaccinia virus may have contributed in several ways to tumor regression, including oncolysis and induction of inflammation, in addition to activation and expansion of T cells. The specific recombinant VV-gp100 vaccine was necessary for tumor eradication, as evidenced by the failure of VV-OVA and VV-Flu to synergize with CARaMEL T cells to induce complete tumor regressions. There are reports of the safe intravenous delivery of oncolytic vaccinia virus to humans, supporting the feasibility of ACTIV therapy (45). However, a range of other recombinant oncolytic viruses exist including adenovirus, herpesvirus and reovirus (46), which may be effective against a variety of cancers depending on viral tropism for, and ability to proliferate in, specific tumors.

We also determined that high dose IL-2 was necessary for tumor eradication, and a lymphodepleting preconditioning step has also been shown to be necessary in previous studies using pMEL T cells in the melanoma setting (24). IL-2 played a role in supporting T cell growth and activation, and endogenous IL-2 produced from CARaMEL T cells seemed insufficient for durable tumor eradication. Activation and expansion of $CD8^+$ T cells often benefits from IL-2 secretion from "helper" $CD4^+$ T cells (47). However, the transferred CARaMEL T cells are largely $CD8^+$, which produce little IL-2, suggesting that administration of exogenous IL-2 is required for optimal antitumor activity.

Although IL-2 has been demonstrated to be less well tolerated in humans, similar $CD8^+$ T cell support roles can be attributed to IL-7, IL-15 and IL-21 (41), which may provide less toxic alternate cytokines for T cell support in humans. While both IL-2 and vaccination were necessary for optimal antitumor effects, their administration was not sufficient for tumor eradication, which required co-administration of dual-specific T cells (Fig. 1A,D, Fig. 2A,B). It is likely that the increased frequency

of tumor-specific T cells afforded by this approach contributed to the enhanced efficacy compared to the combination of vaccination and IL-2 therapy.

The lymphodepleting whole body irradiation regimen enhances homeostatic engraftment of T cells and induces systemic inflammatory cytokines through exposure to gut commensal bacteria (48).Thus, in this study, four constituents of ACTIV therapy combined to stimulate immunity leading to tumor destruction.

Of note was the ability of ACTIV therapy to eradicate tumors of several different histologies and in different tissues. Tumors of different histologies can vary in the composition of their immunosuppressive microenvironments, which can affect their response to immunotherapy (49, 50). Indeed, tumors of different types and in various anatomical locations vary in their response to immunotherapy (51). Our results in several models suggest that inducing a robust immune response has the ability to overcome a variety of immunosuppressive mechanisms leading to the resolution of established malignant disease.

In addition to demonstrating the outstanding efficacy of this approach, we also identified some unique mechanistic insight into the role of IFN-γ. In contrast to many previous studies indicating an essential role for IFN-γ in cancer immunotherapy (42), we demonstrated a reduced contribution of IFN-γ to ACTIV therapy. However, we did observe enhanced activity of vaccinia virus, as seen by the appearance of small lesions on the tails of mice that were administered IFN-γ-neutralizing antibody. It is therefore possible that any direct decrease in T cell function mediated by reduced IFN-γ was offset by enhanced activity of vaccinia virus. The appearance of viral lesions suggests at least partial inhibition of interferon, but it is not clear at this stage whether neutralization of IFN-γ was complete.

CXCR3 is a chemokine receptor expressed on activated T cells, particularly Th1-type $CD4^+$ T cells and $CD8^+$ cytotoxic T lymphocytes, and is involved in migration of T cells towards tumors (52)

and viral infected tissues (53). Here, we demonstrated the importance of CXCR3 in eradicating tumors using adoptively transferred dual-specific T cells.

Our observations that mice that had rejected $Her2^{+}$ tumors were resistant to rechallenge with the same tumor lacking Her2 suggested that ACTIV therapy had assisted in the generation of an immune response against tumor antigens other than Her2 in a process referred to as determinant- or epitope-spreading (54). In addition, we observed that mice surviving after primary tumor rejection were partially resistant to rechallenge with different tumors that shared Her2 expression, but not other antigens, with the primary tumor. Epitope spreading has been observed previously in patients receiving ACT as evidenced by the appearance of new antibody specificities (55) and increased frequency of T cells specific for several candidate antigens (56). Here, we provide further support for the ability of ACT to induce epitope spreading. In addition, we provide evidence that this phenomenon, induced as a result of combined CAR T cell and vaccine, can potentially participate in the rejection of tumors and protection from disease recurrence.

In this study, we targeted the tumor-associated antigen Her2 using CAR T cells, but the availability of CARs of other specificities enables the extension of this approach to wide variety of antigens. Furthermore, primarily for modelling purposes, we used a TCR specific for gp100, which is an antigen expressed in normal human tissues including melanocytes, substantia nigra and retina. The use of this TCR in the clinic would not be ideal due to potential toxicity against normal tissues. A clinically safer option would be to develop TCRs specific for foreign antigens such as influenza virus. In addition, the development of further TCRs would extend specificities beyond the HLA-A*0201 restriction of the current model.

Previous studies have utilized CAR-transduced virus-specific T cells bearing an endogenous virus-specific TCR reactive with Epstein-Barr virus or cytomegalovirus or adenovirus (57-59). While these T cells possessed activity against both viral antigens and tumor, they did not expand well after adoptive transfer. In contrast, dual-specific T cells in the current study expanded extensively,

suggesting that expansion of transferred T cells may be better achieved using active administration of a potent viral vaccine rather than relying on stimulation by endogenous reserves of persisting virus.

Tumor-associated antigens are often expressed by a range of normal tissues and on-target/off-tumor toxicities have been observed in some previous clinical trials using CAR T cells (60-62). We observed toxicity in Her2 transgenic mice receiving ACTIV therapy, manifested by weight loss, lethargy and unsteady movement. Our observations of a role for Her2 expression in the brain in mediating infiltration into the cerebellum suggest that an initial low level of predecessor immigrant T cells react against Her2 to either create an inflammatory environment to attract more T cells, or their proliferation in situ, or a combination of these events. However, toxicity was not observed in mice receiving ACTIV therapy where pMEL T cells substituted for CARaMEL T cells or in $RAG1^{-/-}$ mice that lacked Her2 expression in normal tissues. This suggested that a direct response against Her2-expressing normal tissues, most likely brain, was the predominant contributing factor to toxicity.

This mouse model in which Her2 was expressed in brain and breast provided valuable insight into targeting a tumor-associated antigen using CAR T cells. We observed that large tumor burdens could be eliminated despite considerable self-antigen expression, even in crucial tissues, with limited transient toxicity. Thus, while the initial promise of greater specificity and less toxicity of immunotherapies has yet to be realized, this study in the challenging solid tumor setting, together with other studies in hematologic cancers, have identified promising ways to eradicate malignancies, albeit with some toxicity (10-13). Future developments of these approaches, particularly using logic-gated chimeric receptors (63, 64), with two or more specificities, may yet see truly tumor-specific immunotherapies free of side effects come to fruition.

The wider clinical application of the approach may involve transduction of patient T cells with two genes, one encoding a CAR and one encoding a TCR of known specificity. Alternatively, it may be possible to design potent vaccines to use with CAR-modified viral-specific T cells to build on previous approaches (58).

Our results support a view that it is possible to design an effective combination immunotherapy approach such that tumor destruction occurs, along with tolerable side effects, when each component cooperates to induce optimal effects, as seen in this study using a combination of dual-specific CAR T cells and an indirect vaccine.

Acknowledgements: The authors would like to acknowledge the assistance of Dr William Murray (Pathologist) and Ben Venville (Senior Animal Technician).

Author contributions: C.Y.S., P.K.D and M.H.K. conceived, designed and performed experiments, analysed data and wrote the manuscript. B.V.S., A.A., A.J.D., P.A.B., J.A.W., S.M. performed experiments. D.C.T. and S.E. provided important reagents, protocols and data analysis. H.M.P., J.A.T., R.W.J., M.J.S., M.W.T. and P.N. provided intellectual input into study design and data interpretation. Z.Y., S.A.R. and N.P.R. provided important reagents, protocols and intellectual input.

REFERENCES:

1. Restifo NP, Dudley ME, Rosenberg SA. Adoptive immunotherapy for cancer: harnessing the T cell response. Nat Rev Immunol. 2012;12:269-81.
2. Hinrichs CS, Rosenberg SA. Exploiting the curative potential of adoptive T-cell therapy for cancer. Immunol Rev. 2014;257:56-71.
3. Ellebaek E, Iversen TZ, Junker N, Donia M, Engell-Noerregaard L, Met O, et al. Adoptive cell therapy with autologous tumor infiltrating lymphocytes and low-dose Interleukin-2 in metastatic melanoma patients. J Transl Med. 2012;10:169.
4. Itzhaki O, Hovav E, Ziporen Y, Levy D, Kubi A, Zikich D, et al. Establishment and large-scale expansion of minimally cultured "young" tumor infiltrating lymphocytes for adoptive transfer therapy. J Immunother. 2011;34:212-20.
5. Radvanyi LG, Bernatchez C, Zhang M, Fox PS, Miller P, Chacon J, et al. Specific lymphocyte subsets predict response to adoptive cell therapy using expanded autologous tumor-infiltrating lymphocytes in metastatic melanoma patients. Clin Cancer Res. 2012;18:6758-70.
6. Heslop HE, Slobod KS, Pule MA, Hale GA, Rousseau A, Smith CA, et al. Long-term outcome of EBV-specific T-cell infusions to prevent or treat EBV-related lymphoproliferative disease in transplant recipients. Blood. 2010;115:925-35.
7. Yannelli JR, Hyatt C, McConnell S, Hines K, Jacknin L, Parker L, et al. Growth of tumor-infiltrating lymphocytes from human solid cancers: summary of a 5-year experience. Int J Cancer. 1996;65:413-21.
8. Kershaw MH, Westwood JA, Darcy PK. Gene-engineered T cells for cancer therapy. Nat Rev Cancer. 2013;13:525-41.
9. Kershaw MH, Teng MW, Smyth MJ, Darcy PK. Supernatural T cells: genetic modification of T cells for cancer therapy. Nat Rev Immunol. 2005;5:928-40.
10. Davila ML, Riviere I, Wang X, Bartido S, Park J, Curran K, et al. Efficacy and toxicity management of 19-28z CAR T cell therapy in B cell acute lymphoblastic leukemia. Sci Transl Med. 2014;6:224ra25.
11. Kochenderfer JN, Dudley ME, Kassim SH, Somerville RP, Carpenter RO, Stetler-Stevenson M, et al. Chemotherapy-Refractory Diffuse Large B-Cell Lymphoma and Indolent B-Cell Malignancies Can Be Effectively Treated With Autologous T Cells Expressing an Anti-CD19 Chimeric Antigen Receptor. J Clin Oncol. 2014.
12. Lee DW, Kochenderfer JN, Stetler-Stevenson M, Cui YK, Delbrook C, Feldman SA, et al. T cells expressing CD19 chimeric antigen receptors for acute lymphoblastic leukaemia in children and young adults: a phase 1 dose-escalation trial. Lancet. 2014.
13. Maude SL, Frey N, Shaw PA, Aplenc R, Barrett DM, Bunin NJ, et al. Chimeric antigen receptor T cells for sustained remissions in leukemia. N Engl J Med. 2014;371:1507-17.
14. Adusumilli PS, Cherkassky L, Villena-Vargas J, Colovos C, Servais E, Plotkin J, et al. Regional delivery of mesothelin-targeted CAR T cell therapy generates potent and long-lasting CD4-dependent tumor immunity. Sci Transl Med. 2014;6:261ra151.
15. Carpenito C, Milone MC, Hassan R, Simonet JC, Lakhal M, Suhoski MM, et al. Control of large, established tumor xenografts with genetically retargeted human T cells containing CD28 and CD137 domains. Proc Natl Acad Sci U S A. 2009;106:3360-5.
16. Posey AD, Jr., Schwab RD, Boesteanu AC, Steentoft C, Mandel U, Engels B, et al. Engineered CAR T Cells Targeting the Cancer-Associated Tn-Glycoform of the Membrane Mucin MUC1 Control Adenocarcinoma. Immunity. 2016;44:1444-54.
17. Wang LX, Westwood JA, Moeller M, Duong CP, Wei WZ, Malaterre J, et al. Tumor ablation by gene-modified T cells in the absence of autoimmunity. Cancer Res. 2010;70:9591-8.

18. Chmielewski M, Hahn O, Rappl G, Nowak M, Schmidt-Wolf IH, Hombach AA, et al. T cells that target carcinoembryonic antigen eradicate orthotopic pancreatic carcinomas without inducing autoimmune colitis in mice. Gastroenterology. 2012;143:1095-107 e2.
19. John LB, Devaud C, Duong CP, Yong CS, Beavis PA, Haynes NM, et al. Anti-PD-1 antibody therapy potently enhances the eradication of established tumors by gene-modified T cells. Clin Cancer Res. 2013;19:5636-46.
20. Kershaw MH, Westwood JA, Hwu P. Dual-specific T cells combine proliferation and antitumor activity. Nat Biotechnol. 2002;20:1221-7.
21. Murphy A, Westwood JA, Brown LE, Teng MW, Moeller M, Xu Y, et al. Antitumor activity of dual-specific T cells and influenza virus. Cancer Gene Ther. 2007;14:499-508.
22. Kershaw MH, Westwood JA, Parker LL, Wang G, Eshhar Z, Mavroukakis SA, et al. A phase I study on adoptive immunotherapy using gene-modified T cells for ovarian cancer. Clin Cancer Res. 2006;12:6106-15.
23. Wen FT, Thisted RA, Rowley DA, Schreiber H. A systematic analysis of experimental immunotherapies on tumors differing in size and duration of growth. Oncoimmunology. 2012;1:172-8.
24. Overwijk WW, Theoret MR, Finkelstein SE, Surman DR, de Jong LA, Vyth-Dreese FA, et al. Tumor regression and autoimmunity after reversal of a functionally tolerant state of self-reactive CD8+ T cells. J Exp Med. 2003;198:569-80.
25. Yong CS, Westwood JA, Schroder J, Papenfuss AT, von Scheidt B, Moeller M, et al. Expression of a Chimeric Antigen Receptor in Multiple Leukocyte Lineages in Transgenic Mice. PLoS One. 2015;10:e0140543.
26. Piechocki MP, Ho YS, Pilon S, Wei WZ. Human ErbB-2 (Her-2) transgenic mice: a model system for testing Her-2 based vaccines. J Immunol. 2003;171:5787-94.
27. Johnstone CN, Smith YE, Cao Y, Burrows AD, Cross RS, Ling X, et al. Functional and molecular characterisation of EO771.LMB tumours, a new C57BL/6-mouse-derived model of spontaneously metastatic mammary cancer. Disease models & mechanisms. 2015;8:237-51.
28. Shiloni E, Karp SE, Custer MC, Shilyansky J, Restifo NP, Rosenberg SA, et al. Retroviral transduction of interferon-gamma cDNA into a nonimmunogenic murine fibrosarcoma: generation of T cells in draining lymph nodes capable of treating established parental metastatic tumor. Cancer Immunol Immunother. 1993;37:286-92.
29. Corbett TH, Griswold DP, Jr., Roberts BJ, Peckham JC, Schabel FM, Jr. Tumor induction relationships in development of transplantable cancers of the colon in mice for chemotherapy assays, with a note on carcinogen structure. Cancer Res. 1975;35:2434-9.
30. Moeller M, Haynes NM, Trapani JA, Teng MW, Jackson JT, Tanner JE, et al. A functional role for CD28 costimulation in tumor recognition by single-chain receptor-modified T cells. Cancer Gene Ther. 2004;11:371-9.
31. Overwijk WW, Tsung A, Irvine KR, Parkhurst MR, Goletz TJ, Tsung K, et al. gp100/pmel 17 is a murine tumor rejection antigen: induction of "self"-reactive, tumoricidal T cells using high-affinity, altered peptide ligand. J Exp Med. 1998;188:277-86.
32. Lev A, Takeda K, Zanker D, Maynard JC, Dimberu P, Waffarn E, et al. The exception that reinforces the rule: crosspriming by cytosolic peptides that escape degradation. Immunity. 2008;28:787-98.
33. Restifo NP, Bacik I, Irvine KR, Yewdell JW, McCabe BJ, Anderson RW, et al. Antigen processing in vivo and the elicitation of primary CTL responses. J Immunol. 1995;154:4414-22.
34. Earl PL, Moss B, Wyatt LS, Carroll MW. Generation of recombinant vaccinia viruses. Current protocols in molecular biology / edited by Frederick M Ausubel [et al]. 2001;Chapter 16:Unit16 7.
35. Amos SM, Pegram HJ, Westwood JA, John LB, Devaud C, Clarke CJ, et al. Adoptive immunotherapy combined with intratumoral TLR agonist delivery eradicates established melanoma in mice. Cancer Immunol Immunother. 2011;60:671-83.

36. Yong CS, Sharkey J, Duscio B, Venville B, Wei WZ, Jones RF, et al. Embryonic Lethality in Homozygous Human Her-2 Transgenic Mice Due to Disruption of the Pds5b Gene. PLoS One. 2015;10:e0136817.
37. Kalaitsidou M, Kueberuwa G, Schutt A, Gilham DE. CAR T-cell therapy: toxicity and the relevance of preclinical models. Immunotherapy. 2015;7:487-97.
38. van der Stegen SJ, Davies DM, Wilkie S, Foster J, Sosabowski JK, Burnet J, et al. Preclinical in vivo modeling of cytokine release syndrome induced by ErbB-retargeted human T cells: identifying a window of therapeutic opportunity? J Immunol. 2013;191:4589-98.
39. Crompton JG, Sukumar M, Roychoudhuri R, Clever D, Gros A, Eil RL, et al. Akt inhibition enhances expansion of potent tumor-specific lymphocytes with memory cell characteristics. Cancer Res. 2015;75:296-305.
40. Forget MA, Huon Y, Reuben A, Grange C, Liberman M, Martin J, et al. Stimulation of Wnt/ss-catenin pathway in human CD8+ T lymphocytes from blood and lung tumors leads to a shared young/memory phenotype. PLoS One. 2012;7:e41074.
41. Klebanoff CA, Gattinoni L, Palmer DC, Muranski P, Ji Y, Hinrichs CS, et al. Determinants of successful CD8+ T-cell adoptive immunotherapy for large established tumors in mice. Clin Cancer Res. 2011;17:5343-52.
42. Uno T, Takeda K, Kojima Y, Yoshizawa H, Akiba H, Mittler RS, et al. Eradication of established tumors in mice by a combination antibody-based therapy. Nat Med. 2006;12:693-8.
43. Wang B, Norbury CC, Greenwood R, Bennink JR, Yewdell JW, Frelinger JA. Multiple paths for activation of naive CD8+ T cells: CD4-independent help. J Immunol. 2001;167:1283-9.
44. Gammon DB, Gowrishankar B, Duraffour S, Andrei G, Upton C, Evans DH. Vaccinia virus-encoded ribonucleotide reductase subunits are differentially required for replication and pathogenesis. PLoS Pathog. 2010;6:e1000984.
45. Breitbach CJ, Burke J, Jonker D, Stephenson J, Haas AR, Chow LQ, et al. Intravenous delivery of a multi-mechanistic cancer-targeted oncolytic poxvirus in humans. Nature. 2011;477:99-102.
46. Kaufman HL, Kohlhapp FJ, Zloza A. Oncolytic viruses: a new class of immunotherapy drugs. Nat Rev Drug Discov. 2015;14:642-62.
47. Boyman O, Sprent J. The role of interleukin-2 during homeostasis and activation of the immune system. Nat Rev Immunol. 2012;12:180-90.
48. Paulos CM, Wrzesinski C, Kaiser A, Hinrichs CS, Chieppa M, Cassard L, et al. Microbial translocation augments the function of adoptively transferred self/tumor-specific CD8+ T cells via TLR4 signaling. J Clin Invest. 2007;117:2197-204.
49. Devaud C, John LB, Westwood JA, Darcy PK, Kershaw MH. Immune modulation of the tumor microenvironment for enhancing cancer immunotherapy. Oncoimmunology. 2013;2:e25961.
50. Gajewski TF. The Next Hurdle in Cancer Immunotherapy: Overcoming the Non-T-Cell-Inflamed Tumor Microenvironment. Seminars in oncology. 2015;42:663-71.
51. Devaud C, Westwood JA, John LB, Flynn JK, Paquet-Fifield S, Duong CP, et al. Tissues in different anatomical sites can sculpt and vary the tumor microenvironment to affect responses to therapy. Mol Ther. 2014;22:18-27.
52. Slaney CY, Kershaw MH, Darcy PK. Trafficking of T cells into tumors. Cancer Res. 2014;74:7168-74.
53. Hickman HD, Reynoso GV, Ngudiankama BF, Cush SS, Gibbs J, Bennink JR, et al. CXCR3 chemokine receptor enables local CD8(+) T cell migration for the destruction of virus-infected cells. Immunity. 2015;42:524-37.
54. Ribas A, Timmerman JM, Butterfield LH, Economou JS. Determinant spreading and tumor responses after peptide-based cancer immunotherapy. Trends Immunol. 2003;24:58-61.

55. Beatty GL, Haas AR, Maus MV, Torigian DA, Soulen MC, Plesa G, et al. Mesothelin-specific chimeric antigen receptor mRNA-engineered T cells induce anti-tumor activity in solid malignancies. Cancer immunology research. 2014;2:112-20.
56. Bollard CM, Gottschalk S, Torrano V, Diouf O, Ku S, Hazrat Y, et al. Sustained complete responses in patients with lymphoma receiving autologous cytotoxic T lymphocytes targeting Epstein-Barr virus latent membrane proteins. J Clin Oncol. 2014;32:798-808.
57. Cruz CR, Micklethwaite KP, Savoldo B, Ramos CA, Lam S, Ku S, et al. Infusion of donor-derived CD19-redirected virus-specific T cells for B-cell malignancies relapsed after allogeneic stem cell transplant: a phase 1 study. Blood. 2013;122:2965-73.
58. Louis CU, Savoldo B, Dotti G, Pule M, Yvon E, Myers GD, et al. Antitumor activity and long-term fate of chimeric antigen receptor-positive T cells in patients with neuroblastoma. Blood. 2011;118:6050-6.
59. Pule MA, Savoldo B, Myers GD, Rossig C, Russell HV, Dotti G, et al. Virus-specific T cells engineered to coexpress tumor-specific receptors: persistence and antitumor activity in individuals with neuroblastoma. Nat Med. 2008;14:1264-70.
60. Lamers CH, Sleijfer S, Vulto AG, Kruit WH, Kliffen M, Debets R, et al. Treatment of metastatic renal cell carcinoma with autologous T-lymphocytes genetically retargeted against carbonic anhydrase IX: first clinical experience. J Clin Oncol. 2006;24:e20-2.
61. Morgan RA, Yang JC, Kitano M, Dudley ME, Laurencot CM, Rosenberg SA. Case report of a serious adverse event following the administration of T cells transduced with a chimeric antigen receptor recognizing ERBB2. Mol Ther. 2010;18:843-51.
62. Grupp SA, Kalos M, Barrett D, Aplenc R, Porter DL, Rheingold SR, et al. Chimeric Antigen Receptor-Modified T Cells for Acute Lymphoid Leukemia. N Engl J Med. 2013.
63. Fedorov VD, Themeli M, Sadelain M. PD-1- and CTLA-4-based inhibitory chimeric antigen receptors (iCARs) divert off-target immunotherapy responses. Sci Transl Med. 2013;5:215ra172.
64. Kloss CC, Condomines M, Cartellieri M, Bachmann M, Sadelain M. Combinatorial antigen recognition with balanced signaling promotes selective tumor eradication by engineered T cells. Nat Biotechnol. 2012;31:71-5.

FIGURE LEGENDS

Figure 1. ACTIV therapy mediates regression of established orthotopic breast tumors. (A) Mice bearing established E0771-Her2 mammary tumors received the treatments listed and tumor growth monitored. **(B)** Tumor growth in individual mice receiving ACTIV therapy from panel (A). **(C)** Example of a mouse bearing a tumor in excess of 150 mm^2 before (left panel) and after (right panel) ACTIV therapy. **(D)** Survival of tumor-bearing mice from panel (A) after receiving the treatments listed (A-D, n=7 mice for CARaMEL + IL-2 and untreated, and 8 mice in all other groups, representative of 3 experiments). **(E)** Tumor growth in mice receiving purified CD4+ or CD8+ CARaMEL T cells or splenocytes that had undergone a mock purification process (E, n=4 for the CD8+ and CD4+ CARaMEL group, n=5 for the CD8+ CARaMEL group and n=6 mice for other groups, representative of 3 experiments). (F) Tumor growth in mice bearing either Her2-positive or Her-2-negative E0771 tumors that were treated with ACTIV therapy or untreated (n=6 mice per group). (G) Mice received either tumor cells expressing Her2 (5×10^5) or not (5×10^4), or a mixture of Her-positive (4.5×10^5) and Her-2-negative (5×10^4) cells. All groups, except non-treated, received human recombinant IL-2 and 5 Gy irradiation according to the standard ACTIV treatment detailed in Materials and Methods. Data is displayed as the mean with error bars representing the SEM. Significance determined by one-way ANOVA (A, E) and Mantel-Cox test (D) *$p<0.05$, **$p<0.01$, ***$p<0.001$, ****$p<0.0001$.

Figure 2. A variety of solid tumors respond to ACTIV therapy. (A) Tumor growth in mice bearing established (14-day) subcutaneous 24JK-Her2 fibrosarcomas receiving ACTIV therapy (5 Gy irradiation + VV-gp100 + CARaMEL + IL-2) or treatment where pMEL T cells substituted for CARaMEL T cells (n=7 mice per group, representative of two experiments). **(B)** Tumor growth in mice bearing established (14-day) subcutaneous MC38-Her2 colon carcinomas (n=5 for the CARaMEL group and n=6 mice for the rest of the groups, representative of two experiments and **(C)** Survival of

mice bearing established (11-day) MC38-Her2 subcutaneous tumors. **(D)** Representative pictures of mice bearing MC38-Her2 liver tumors before treatment (left panel) or 7 days later after receiving no treatment (center panel) or 100 days post ACTIV treatment (right panel)(arrow points to large hepatic tumor) (C and D, n=9 mice for ACTIV-treated, n=10 for untreated). (E) Survival of mice bearing established (11 day) MC38-Her2 liver tumors. (F) Tumor growth in mice bearing subcutaneous 24JK tumors lacking Her2 expression and either ACTIV-treated or non-treated (n=6 mice per group). (G) Tumor growth in mice bearing subcutaneous MC38 tumors lacking Her2 expression and either ACTIV-treated or non-treated (n=6 mice per group). All treated groups of mice received human recombinant IL-2 and 5 Gy irradiation according to the standard ACTIV treatment detailed in Materials and Methods. Data is displayed as the mean with error bars representing the SEM. Significance determined using one-way ANOVA (A,B) and Mantel-Cox test (C) **p<0.01, ***p<0.001, ****p<0.0001.

Figure 3. Specific vaccinia virus and dual-specific T cells are required for optimal anti-tumor activity. (A) E0771-Her2 tumor growth in mice receiving ACTIV therapy (5 Gy irradiation + VV-gp100+CARaMEL+IL-2) or treatments containing viruses lacking gp100 (n=6 mice per group). **(B)** Mice received either T cells expressing the Her2-specific CAR and an ovalbumin-specific TCR (CAROT T cells) instead of CARaMEL T cells, or a mixture of T cells from CAR mice and pMEL mice (pMEL+CAR, 1 x 10^7 of each), in which the Her2-specific CAR and the gp100-specific TCR were not expressed in the same cell (n=5 mice for VV-gp100 treated group, n=6 for all other groups). All treated mice in this figure received IL-2 and 5 Gy irradiation. Data is displayed as the mean with error bars representing the SEM. Significance determined by one-way ANOVA *p<0.05, **p<0.01.

Figure 4. ACTIV therapy leads to expansion of T cells and their accumulation in tumors. (A) Spleens and **(B)** E0771-Her2 tumors, were taken at the listed time points and subjected to flow

cytometric analysis. The percentage of $CD8^+/Thy1.1^+$ live cells is presented (For A, n=3 mice for Day 3, n=6 mice for all other groups. For B, n=6 mice per group. Representative of 3 experiments). **(C)** Representative sections of tumors from mice treated with ACTIV therapy (lower panel) or therapy lacking vaccinia (upper panel) stained with anti-CD8 (brown) (scale bar = 50 μm) (Representative of tumors from 3 mice, 3 sections per mouse). **(D)** Representative flow cytometry plots gated on $CD8^+/Thy1.1^+$ from spleens and tumors of mice receiving either ACTIV therapy (lower panel) or therapy lacking vaccinia (upper panel) stained with anti-IFN-γ and anti-CD44 (n=3 mice per group). (E) Representative flow cytometry plots of dissociated tumors from mice receiving $Thy1.1^+$ T cells possessing both the CAR and pMEL (CARaMEL) or the pMEL TCR alone (pMEL). All treated mice in this figure received IL-2 and 5 Gy irradiation. Data is displayed as the mean with error bars representing the SEM. Significance determined using Student's t test (two-sided) (a,b) **p<0.01, ***p<0.001, ****p<0.0001.

Figure 5. Surviving mice are resistant to tumor rechallenge. Mice that had rejected **(A)** E0771-Her2, **(B)** MC38-Her2, **(C)** 24JK-Her2 following ACTIV therapy were rechallenged with E0771-Her2 or MC38-Her2 or 24JK-Her2 respectively and tumor growth compared to that in naïve mice (control) (n=4 mice per group). Mice that had rejected **(D)** E0771-Her2, **(E)** MC38-Her2, **(F)** 24JK-Her2 were rechallenged with E0771 or MC38 or 24JK cells (lacking Her2) respectively and tumor growth compared to that in naïve mice (control) (n=4 mice per group). Mice that had rejected E0771-Her2 were rechallenged with **(G)** MC38-Her2 or **(H)** 24JK-Her2 and tumor growth compared to that in control naïve mice (n=5 mice per group). Mice that had rejected E0771-Her2 were rechallenged with **(I)** MC38 (lacking Her2) or **(J)** 24JK (lacking Her2) and tumor growth compared to that in control

naïve mice (n=5 mice per group). Data is displayed as the mean with error bars representing the SEM. Significance determined by Mann-Whitney test. *p<0.05, **p<0.01, ***p<0.001, ****p<0.0001.

Figure 6. Dual-specific T cells accumulate in Her2-expressing normal tissues. (A)-(C) CD8-stained (in brown) breast tissue taken from **(A)** lactating mice receiving ACTIV therapy or from **(B)** naïve mice or from **(C)** non-lactating mice receiving ACTIV therapy. **(D)** Section of cerebellum from control E0771-Her2 tumor-bearing mice and **(E)** cerebellum from ACTIV-treated mice and **(F)** cerebrum from ACTIV-treated mice all stained with anti-CD8. **(G) and (H)** cerebellums from $RAG1^{-/-}$ mice or Her2 transgenic mice respectively stained with anti-Her2. **(I)** CD8-stained cerebellum from $RAG1^{-/-}$ mice 5 days after ACTIV treatment. **(J)** Cerebellum of Her2 transgenic mouse >60 days after ACTIV therapy and tumor rejection. **(K)** body weight of E0771-Her2 tumor-bearing $RAG1^{-/-}$ or Her2 mice receiving ACTIV therapy or non-treated. **(L)** E0771-Her2 tumor growth in either $RAG1^{-/-}$ or Her2 mice receiving ACTIV therapy or non-treated. (A) – (J) representative of 3 sections from each of 3 mice. (K) and (L) $RAG1^{-/-}$ control=7 mice, $RAG1^{-/-}$ ACTIV=8 mice, Her2 control=8 mice, Her2 ACTIV=6 mice. All treated mice received the full ACTIV therapy regimen including human recombinant IL-2 as described in Material and Methods. Data is displayed as the mean with error bars representing the SEM. Significance determined using one-way ANOVA. **p<0.01, ****p<0.0001, ns – not significant. Scale bar = 50 μm.

Figure 1

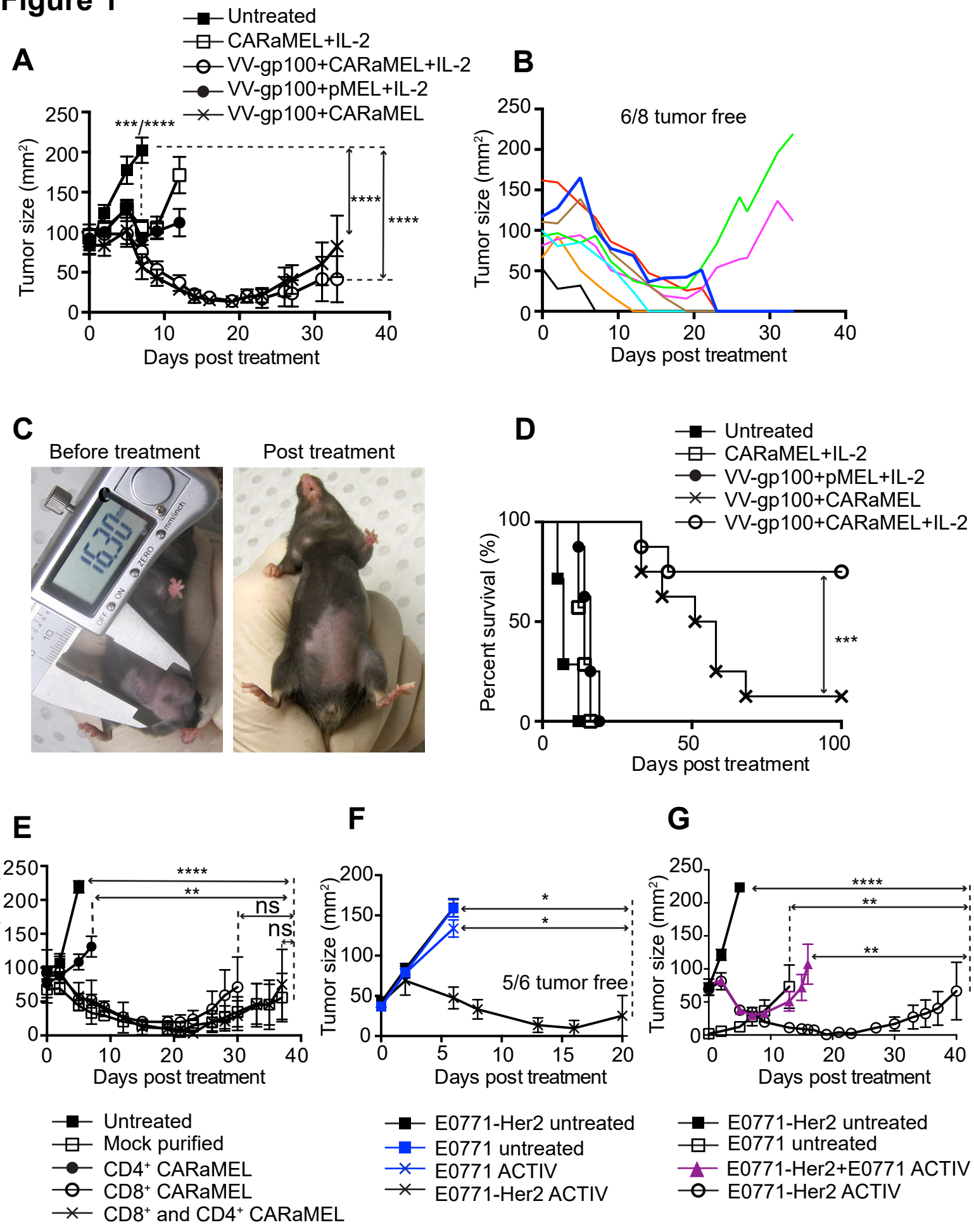
A
Untreated
CARaMEL+IL-2
VV-gp100+CARaMEL+IL-2
VV-gp100+pMEL+IL-2
VV-gp100+CARaMEL
/*
****
****
Tumor size (mm²)
Days post treatment
B
6/8 tumor free
Tumor size (mm²)
Days post treatment
C
Before treatment
Post treatment
D
Untreated
CARaMEL+IL-2
VV-gp100+pMEL+IL-2
VV-gp100+CARaMEL
VV-gp100+CARaMEL+IL-2
***
Percent survival (%)
Days post treatment
E
****
**
ns
ns
Tumor size (mm²)
Days post treatment
Untreated
Mock purified
CD4⁺ CARaMEL
CD8⁺ CARaMEL
CD8⁺ and CD4⁺ CARaMEL
F
*
*
5/6 tumor free
Tumor size (mm²)
Days post treatment
E0771-Her2 untreated
E0771 untreated
E0771 ACTIV
E0771-Her2 ACTIV
G
****
**
**
Tumor size (mm²)
Days post treatment
E0771-Her2 untreated
E0771 untreated
E0771-Her2+E0771 ACTIV
E0771-Her2 ACTIV

Figure 2

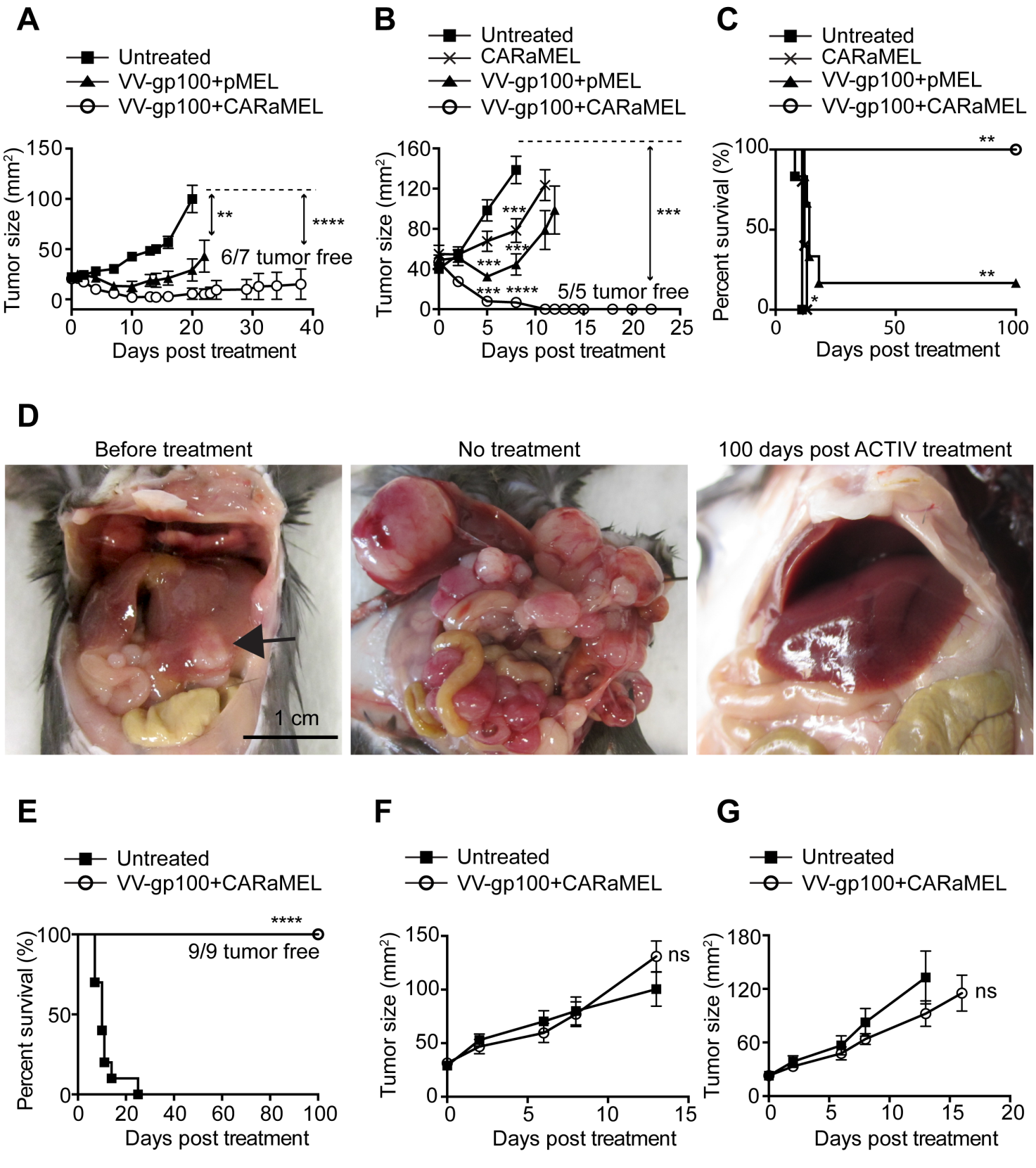
A
Untreated
VV-gp100+pMEL
VV-gp100+CARaMEL
Tumor size (mm²)
Days post treatment
**
****
6/7 tumor free
B
Untreated
CARaMEL
VV-gp100+pMEL
VV-gp100+CARaMEL
Tumor size (mm²)
Days post treatment
***
****
5/5 tumor free
C
Untreated
CARaMEL
VV-gp100+pMEL
VV-gp100+CARaMEL
Percent survival (%)
Days post treatment
**
*
D
Before treatment
No treatment
100 days post ACTIV treatment
1 cm
E
Untreated
VV-gp100+CARaMEL
Percent survival (%)
Days post treatment
****
9/9 tumor free
F
Untreated
VV-gp100+CARaMEL
Tumor size (mm²)
Days post treatment
ns
G
Untreated
VV-gp100+CARaMEL
Tumor size (mm²)
Days post treatment
ns

Figure 3

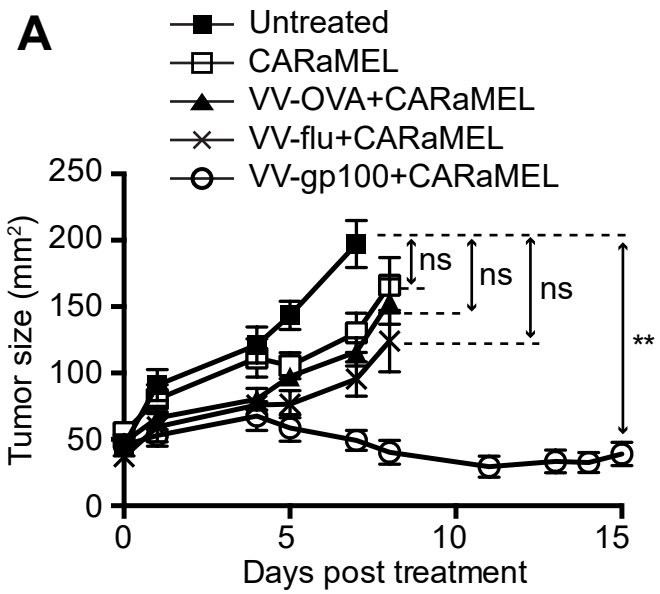
A
Untreated
CARaMEL
VV-OVA+CARaMEL
VV-flu+CARaMEL
VV-gp100+CARaMEL
Tumor size (mm²)
250
200
150
100
50
0
0
5
10
15
Days post treatment
ns
ns
ns
**

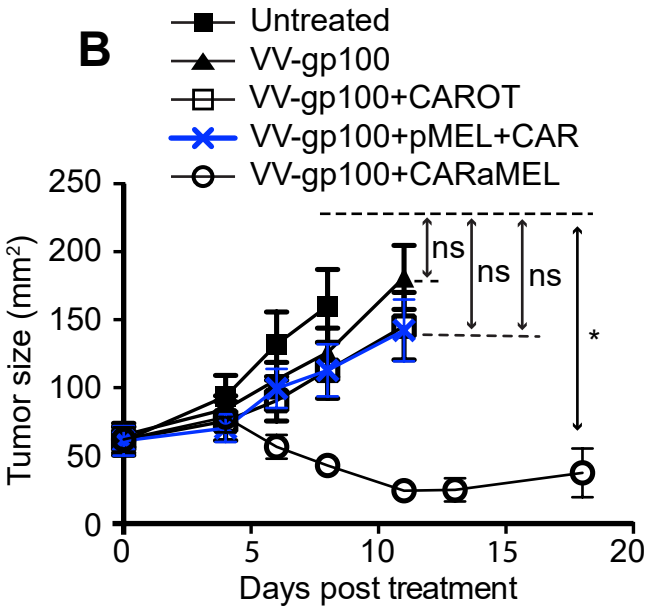
B
Untreated
VV-gp100
VV-gp100+CAROT
VV-gp100+pMEL+CAR
VV-gp100+CARaMEL
Tumor size (mm²)
250
200
150
100
50
0
0
5
10
15
20
Days post treatment
ns
ns
ns
*

Figure 4

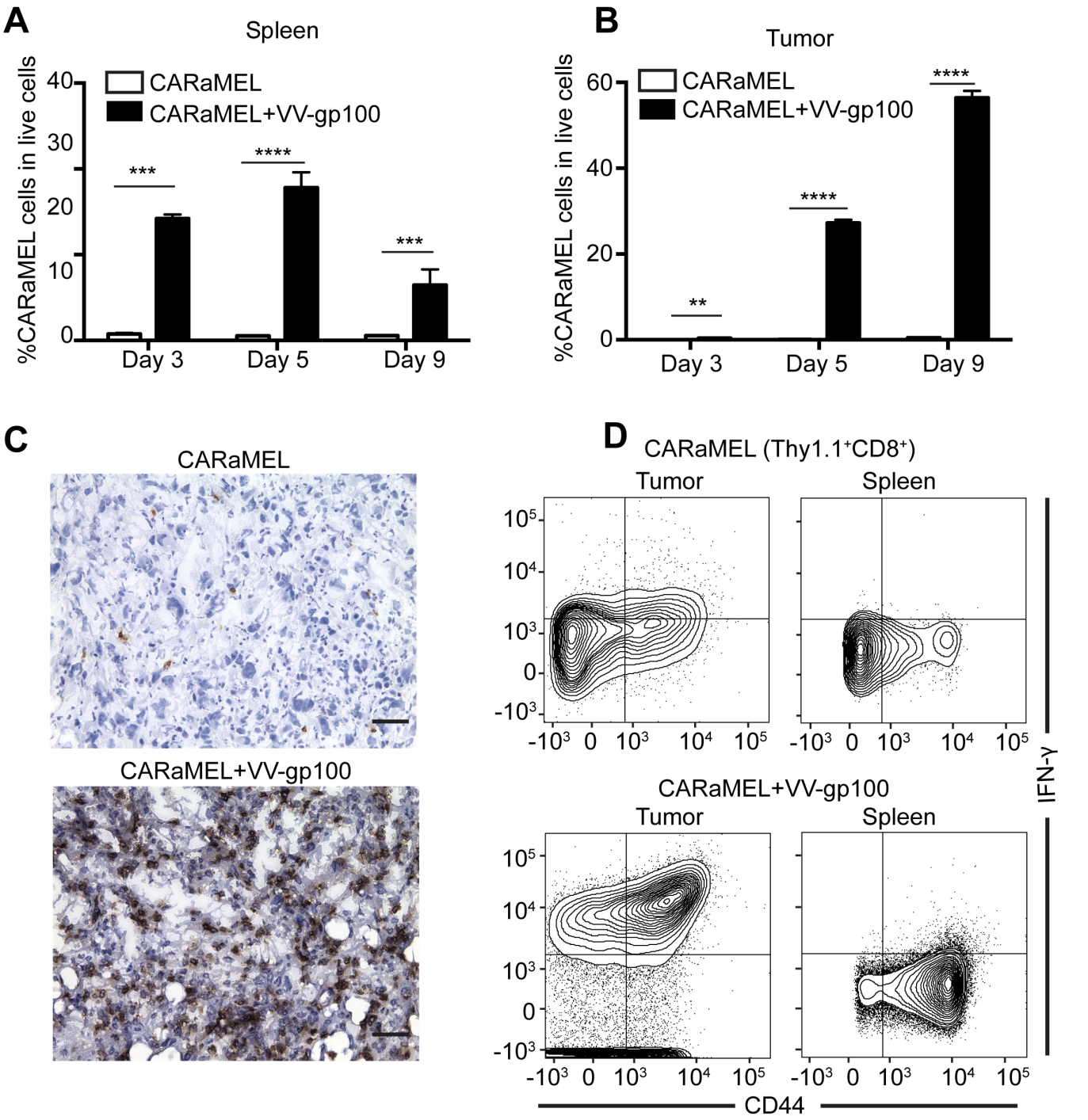
A
Spleen
%CARaMEL cells in live cells
CARaMEL
CARaMEL+VV-gp100
Day 3
Day 5
Day 9
B
Tumor
C
CARaMEL
CARaMEL+VV-gp100
D
CARaMEL (Thy1.1+CD8+)
Tumor
Spleen
IFN-γ
CD44
E
CARaMEL
CARaMEL+VV-gp100
pMEL+VV-gp100
Untreated
0.3%
26.3%
21.3%
0%
Thy1.1
CD8

Figure 5

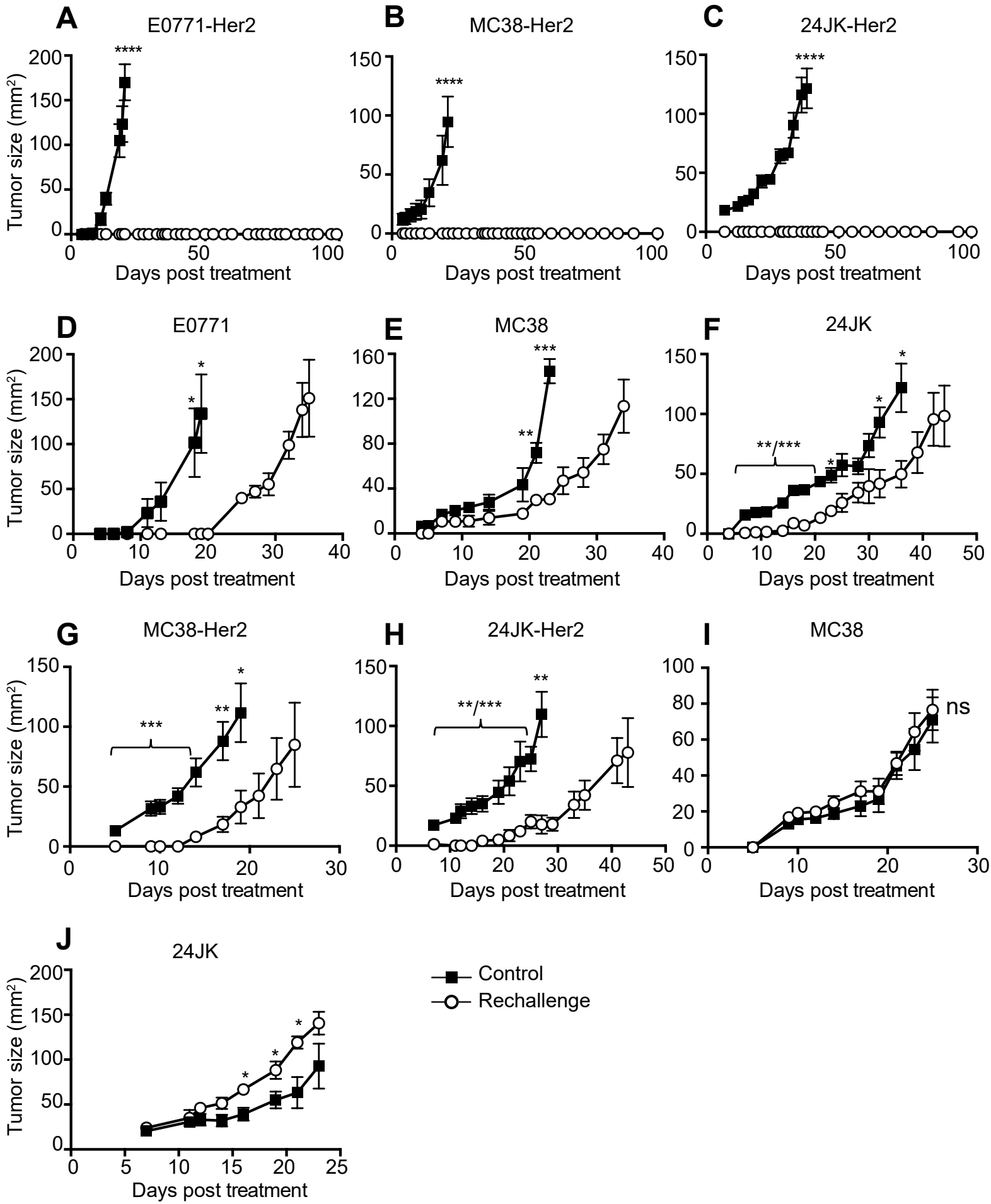
A
E0771-Her2
B
MC38-Her2
C
24JK-Her2
D
E0771
E
MC38
F
24JK
G
MC38-Her2
H
24JK-Her2
I
MC38
J
24JK
Tumor size (mm²)
Days post treatment
****
***
**
*
/*
ns
Control
Rechallenge

Figure 6

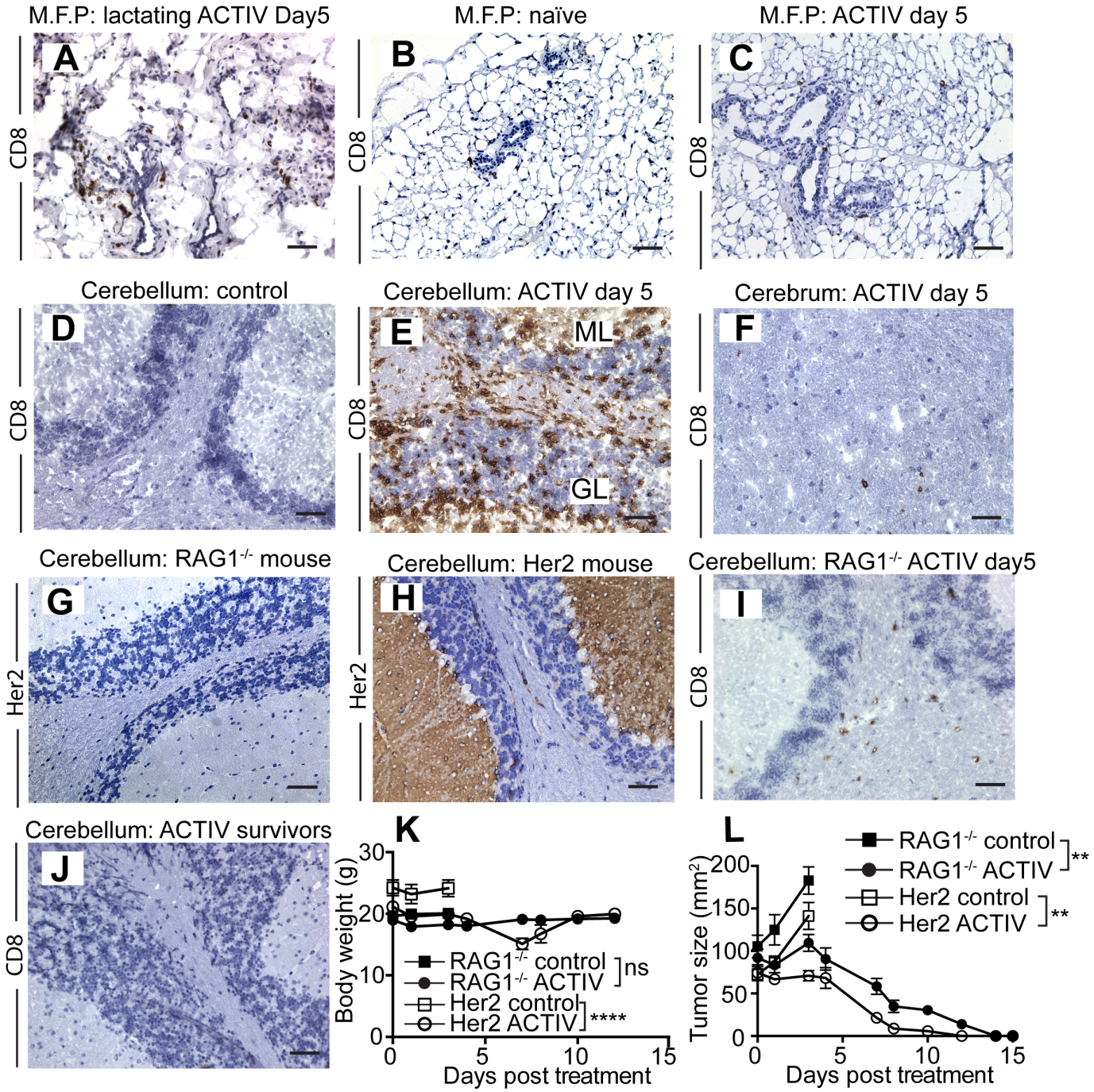
M.F.P: lactating ACTIV Day5
M.F.P: naïve
M.F.P: ACTIV day 5
A
B
C
CD8
Cerebellum: control
Cerebellum: ACTIV day 5
Cerebrum: ACTIV day 5
D
E
F
ML
GL
Cerebellum: RAG1-/- mouse
Cerebellum: Her2 mouse
Cerebellum: RAG1-/- ACTIV day5
G
H
I
Her2
Cerebellum: ACTIV survivors
J
K
L
Body weight (g)
Days post treatment
RAG1-/- control
RAG1-/- ACTIV
Her2 control
Her2 ACTIV
ns
****
Tumor size (mm2)
**
**